Separation Science and Technology
Publication details, including instructions for authors and subscription information:
http://www.informaworld.com/smpp/title~content=t713708471

Adsorption Decontamination of Radioactive Waste Solvent by Activated Alumina and Bauxites

Neguib M. Hassan[a]; Robert S. Matthews[a]; James C. Marra[a]; Edward A. Kyser[a]
[a] WESTINGHOUSE SAVANNAH RIVER CO. SAVANNAH RIVER TECHNOLOGY CENTER, AIKEN, SOUTH CAROLINA

To cite this Article Hassan, Neguib M. , Matthews, Robert S. , Marra, James C. and Kyser, Edward A.(1995) 'Adsorption Decontamination of Radioactive Waste Solvent by Activated Alumina and Bauxites', Separation Science and Technology, 30: 11, 2403 — 2419
To link to this Article: DOI: 10.1080/01496399508013119
URL: http://dx.doi.org/10.1080/01496399508013119

SEPARATION SCIENCE AND TECHNOLOGY, **30**(11), pp. 2403–2419, 1995

Adsorption Decontamination of Radioactive Waste Solvent by Activated Alumina and Bauxites

NEGUIB M. HASSAN,* ROBERT S. MATTHEWS,
JAMES C. MARRA, and EDWARD A. KYSER
WESTINGHOUSE SAVANNAH RIVER CO.
SAVANNAH RIVER TECHNOLOGY CENTER
P.O. BOX 616, AIKEN, SOUTH CAROLINA 29802

ABSTRACT

An adsorption process utilizing activated alumina and activated bauxite adsorbents was evaluated as a function of operating parameters for the removal of low level radioactive contaminants from organic waste solvent generated in the fuel reprocessing facilities and support operations at Savannah River Site. The waste solvent, 30 vol% tributyl phosphate in *n*-paraffin diluent, was degraded due to hydrolysis and radiolysis reactions of tributyl phosphate and *n*-paraffin diluent, producing fission product binding degradation impurities. The process, which has the potential for removing these activity-binding degradation impurities from the solvent, was operated downflow through glass columns packed with activated alumina and activated bauxite adsorbents. Experimental breakthrough curves were obtained under various operating temperatures and flow rates. The results show that the adsorption capacities of activated alumina and activated bauxite were in the order of 10^4 and 10^5 dpm/g of adsorbent, respectively. The performance of the adsorption process was evaluated in terms of dynamic parameters (i.e., adsorption capacity, the height and the efficiency of adsorption zone) in such a way as to maximize the adsorption capacity and to minimize the height of the mass transfer or adsorption zone.

INTRODUCTION

The Purex process has been widely used for reprocessing irradiated nuclear fuel elements. The process is based on multistage countercurrent

* To whom correspondence should be addressed.

solvent extraction to separate uranium (U) and plutonium (Pu) from fission products. The U and Pu are extracted into an organic phase (30% tributyl phosphate by volume in *n*-paraffin diluent), leaving the bulk of the fission products in the aqueous raffinate. It was widely recognized (1–4) that the tributyl phosphate (TBP) and the *n*-paraffin diluent are degraded due to hydrolytic and radiolytic reactions, forming activity-binding degradation products that can cause product losses, poor separation efficiencies, and emulsions which could interfere with the process operations. Primary degradation products, such as monobutyl phosphate, dibutyl phosphate, phosphoric acid, and butanol, were produced from the hydrolytic and dealkylation reactions of the tributyl phosphate when contacted with nitric acid at relatively high temperatures. Secondary degradation products, such as nitroparaffins, aldehydes, ketones, and carboxylic acids, originated from the radiolytic reactions of the *n*-paraffin diluent when exposed to intensive radiation. The degraded solvent is continuously regenerated in the Purex process by scrubbing with sodium carbonate, sodium hydroxide, phosphoric acid, and/or potassium hydroxide solutions after each pass through the process, and most of the radioactivity belonging to primary degradation products are removed. The washing solutions, however, cannot remove the long-chain organic compounds (secondary degradation products) which tend to remain in the solvent to again complex fission products when the solvent is recycled. Therefore, other methods, such as vacuum distillation, steam stripping, and flash vaporization, have been proposed (5, 6) to remove these degradation products, thus producing *n*-paraffin diluents with low radioactivity levels and small tributyl phosphate residues. These methods, although effective to some extent, are limited by the maximum allowable distillation temperature that could lead to significant decomposition of the TBP tar residues.

Recently, several investigators (7, 8) have proposed adsorption-based techniques to improve the performance of the recycle solvent in the Purex process. These investigators have shown that solid adsorbents, such as activated alumina and base-treated silica gel, have the potential for removing some of the long-chain, activity-binding, degradation products. The objective of this work was to evaluate an adsorption process utilizing activated alumina and activated bauxite for decontamination of severely degraded, radioactive waste solvent. This study was aimed to support the disposal of radioactive waste solvent, which includes the separation of *n*-tributyl phosphate and activity-binding degradation products from the *n*-paraffin diluent, followed by incineration of the diluent and chemical destruction of the *n*-tributyl phosphate. The effects of temperature and flow rate on the process performance were investigated in the study. The process dynamic parameters, such as adsorption capacity and the height and

efficiency of the adsorption zone, were calculated from experimental breakthrough curves. Thermogravimetric analysis were performed to determine the thermal stability of fresh and used activated alumina and bauxite samples.

EXPERIMENTAL SECTION

Materials

The adsorbents used in this study were activated alumina and activated bauxite. The alumina, Type A-2, was supplied by La Roche Chemicals, and the bauxite, Type RI, was provided by Engelhard Chemical Co. The activated alumina was produced from relatively high purity aluminum hydroxide by controlled heating to eliminate most of the water of hydration whereas the activated bauxite was produced by thermal activation of bauxite containing alumina in the form of gibbsite. The major oxide contents of the adsorbents were Al_2O_3, SiO_2, Fe_2O_3, and TiO_2. Physicochemical properties of the adsorbents are shown in Table 1.

The solvents used in this study were radioactively contaminated TBP/*n*-paraffin waste generated from the fuel reprocessing facilities and support operations at Savannah River Site. The "as received" solvents from different facilities were composed of 30 vol% tributyl phosphate in C_{11}–C_{16} *n*-paraffin diluent (see Table 2). The solvents were extensively degraded and discolored during contact with certain aqueous solutions in fuel reprocessing facilities. The discoloration was due to the presence of long-chain organic degradation products that originated from hydrolysis and radiolysis reactions of TBP and *n*-paraffin diluent. A number of analyses (liquid scintillation counting, alpha plate counting, and alpha pulse height analy-

TABLE 1
Physicochemical Properties of Adsorbents (data from manufacturers)

Properties	Activated alumina	Activated bauxite
Composition, wt%:		
Al_2O_3	93.6	77.7
SiO_2	0.02	10.8
F_2O_3	0.02	6.5
TiO_2	0.002	5.0
Na_2O	0.35	—
Particle size, mesh	12 × 32	30 × 60
Bulk density, kg/m^3	675	853
Surface area, m^2/g	310	244.08

TABLE 2
Physicochemical Properties of *n*-Paraffin Diluent

Property	*n*-Paraffin (C_{11}–C_{16})
Composition:	
n-Paraffin, wt%	98
Aromatics, wt%	0.2
Olefins, wt%	0.1
Flash point, °C, min	70
Specific gravity, 25/25°C, max	0.77
Viscosity, cP, 25°C, max	2.0
Disengaging time, s (70% *n*-paraffin, 30% TBP):	
1 M NaOH, s, max	80
1 M HNO_3, s, max	50
Color	Colorless

sis) were performed prior to use of each solvent to determine its gross alpha activity and the type of nuclides present.

Apparatus and Procedure

Experimental apparatus for measuring adsorption breakthrough curves of activity-binding degradation products is shown in Fig. 1. The measurements of experimental breakthrough curves were performed with two glass columns: a smaller column, 13 mm in diameter, was employed to conduct experiments with activated alumina, and a larger column, 25 mm in diameter, was used with activated bauxite. The smaller column was usually packed with 20 g alumina whereas the larger column was packed with approximately 60 g bauxite. The total bed heights were 43 and 23 cm for the 13 and 25 mm diameter columns, respectively. Special care was taken when packing the columns to ensure that the same amount of adsorbent was used per unit length. Prior to each run the adsorbent was regenerated in the column at 180°C for 6 hours. After regeneration, the column was allowed to cool to the desired adsorption temperature and a radioactively contaminated solvent was pumped from a feed flask at constant flow rate and introduced from the top of the column to avoid fluidization and expansion of the bed. Decontaminated effluent samples were collected from the bottom of the column at equal time intervals using a continuous sampling system. The adsorption run was continued until the bed became exhausted as indicated by the changing color of effluent samples which become increasingly yellowish as complete beakthrough was approached. After adsorption was completed, the solvent feed remaining

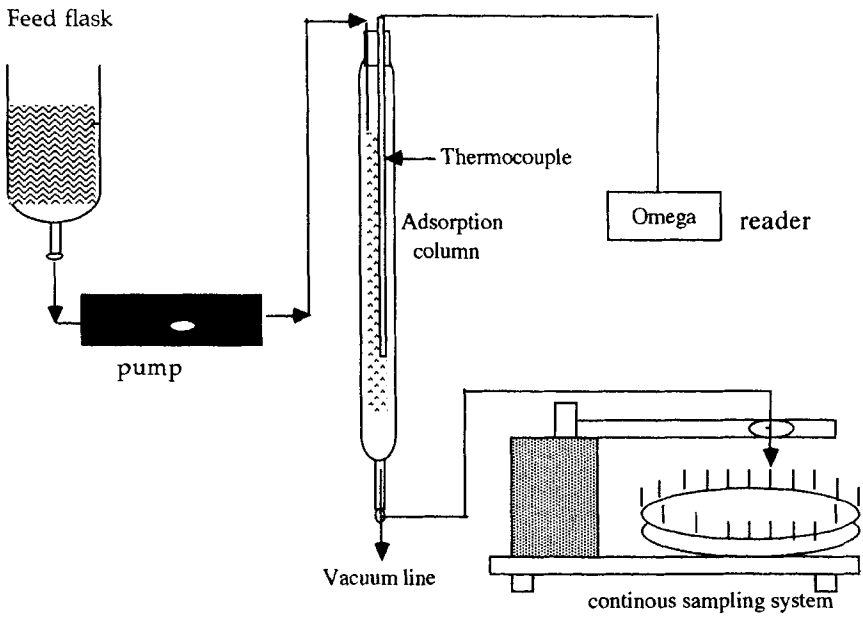

FIG. 1 Schematic diagram of experimental apparatus.

in the bed was drained from the bottom of the column and a small adsorbent sample was removed from the bed for thermogravimetric analysis. The used adsorbent bed was slowly heated while under vacuum to drive off residual volatile material. The dry used bed was finally removed from the column and packed for disposal. All experiments were performed under near-isothermal conditions by controlling the temperature of the surface of the column.

Thermogravimetric Analysis (TGAs)

TGA experiments were performed using a TA Instruments Model 951 thermogravimetric analyzer (TA Instruments, Wilmington, Delaware) coupled with a 2100 thermal analyzer. The unit was installed in a radioactive glovebox and calibrated with a "standard" calcium oxalate monohydrate sample, whose weight loss curves as a function of temperature were known. The TGA curve of the "standard" was used to verify proper temperature calibration and stable instrument operation. After calibration, a clean sample was loaded onto the balance arm and tared by electronic suppression. A small sample, 10 to 28 mg, was then loaded onto the sample

pan and allowed to reach a steady weight at ambient conditions. The sample was heated from room temperature to 1000°C at a rate of 10°C/min, and held at 1000°C for 1 minute. The TGA curve so obtained was used to calculate the percent weight changes in different temperature regions.

Solvent Analysis and Activity Measurement

Three types of analyses [liquid scintillation counting, alpha plate counting, and alpha pulse height analysis (PHA)] were performed with radioactively contaminated feed solvents to determine their gross activity. Liquid scintillation counting (LSC) was used to provide estimates of the residual alpha and beta activities in decontaminated effluent samples. The analysis was performed with Packard Tricarb liquid scintillation counters (Model 2550AB and 2250AC). The samples were properly prepared (i.e., correct volume, cocktail, and vials were chosen), and the gross alpha/beta counting protocol of the instrument was set up to provide the alpha and beta counts in the samples. The sample activity (dpm/mL) was calculated using the net count rate, sample dilution factor, and an average alpha/beta-particle detection efficiency. The precision of this method was found to be $\pm 5\%$ at the 95% confidence level.

The alpha plate counting was used with feed solvents containing significant quantities of alpha/beta activity. A small sample was mounted directly on a metal plate or a dish, and the liquid was evaporated under a heat lamp until it was completely dry. The gross alpha activity on the plate was measured with a gas flow proportional counter; the beta activity was measured with a Geiger-Muller probe. The sample activity (dpm/mL) was calculated from the net count rate of alpha particles, the counting efficiency as determined from an NBS electroplate standard, and the volume of the sample. A precision of $\pm 3\%$ was normally obtained on duplicate alpha plate counting.

The alpha pulse height analysis (PHA) was used to determine the relative count rates of nuclides present within the feed solvent. An alpha spectrophotometer, Model Tennelec TC 256, coupled to a Canberra Series 85 Multichannel analyzer and associated electronics, along with an Si(Au) solid-state surface barrier detector, was used for the alpha PHA measurements. The absolute count rate determined from the gross alpha detector was used in conjunction with the relative percentages of the nuclides present as determined from PHA to ascertain the absolute amount of any alpha-emitting nuclide present.

Theory of Dynamic Adsorption

Mathematical expressions relating dynamic parameters for adsorption to experimental breakthrough curves were used to characterize the ad-

sorption process. The process dynamic parameters studied in this work were the adsorption capacity and the height and efficiency of the adsorption zone. The adsorption zone is a relatively narrow mass transfer band at the top of the bed, where the activity-binding degradation products are initially adsorbed. This zone moves downward through the bed as the solvent flow continues from the top the column and eventually reach the bottom, where the activity-binding degradation products start to break through the column and momentarily appear in the effluent. As the solvent flow continues to the column, the adsorption zone is forced out of the bed and the activity of the effluent samples rapidly approaches that of the feed solvent; the adsorbent bed is considered to be near-saturated. The height of the adsorption zone (h_z) is calculated from the equation by Michael (9):

$$h_z = L_0 \left[\frac{(t_e - t_b)}{(t_e - (1 - F)(t_e - t_b))} \right] \tag{1}$$

where L_0 is the height of adsorbent bed, t_b is the breakthrough time, t_e is the bed exhaustion time, and F is the fraction of the bed that is still capable of adsorbing. The parameter h_z is related to the efficiency of the adsorption zone according to the equation

$$\gamma = \frac{(L_0 - Fh_z)}{L_0} 100 \tag{2}$$

The adsorption capacity, q_m, is determined from the experimental breakthrough by using the equation

$$q_m = \frac{QC_0}{m} \int_{t_b}^{t_e} (1 - C_t/C_0)\, dt \tag{3}$$

where Q is volumetric flow rate, C_0 is the initial activity of the solvent, C_t is the activity of the effluent sample at time t, and m is the mass of adsorbent. The integral in Eq. (3) represents the total area behind the breakthrough curve. The performance of the adsorption decontamination process was evaluated in such a way as to minimize the height of the adsorption zone and to maximize the adsorption capacity.

RESULTS AND DISCUSSION

Thermogravimetric Analysis

Results of the thermogravimetric studies of activated alumina and bauxite samples are shown in Figs. 2 and 3, where TGA curves show the total percent weight change of the samples as a function of temperature. In Fig. 2, the TGA curves of used activated alumina samples obtained from

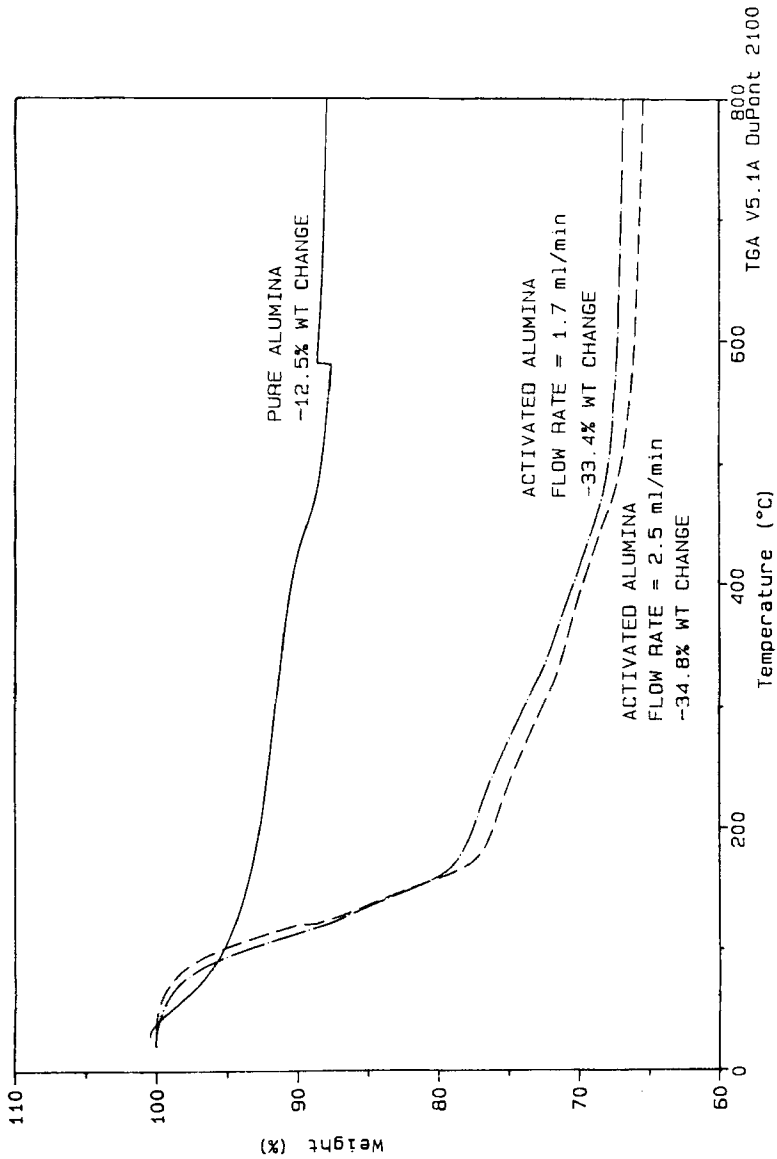

FIG. 2 TGA weight loss curves of activated alumina samples.

adsorption column runs at two different flow rates are presented, along with the TGA curve for fresh activated alumina sample. As can be seen from the figure, the TGA curve for the fresh alumina sample exhibited two plateaus corresponding to weight losses due to dehydration of water molecules (i.e., physisorbed and chemisorbed water) from the alumina surface. The used samples also showed two plateaus, but the weight loss due to desorption of activity-binding degradation products that were adsorbed from the solvent onto the alumina surface was significantly greater than water dehydration. The weight loss for the fresh activated alumina was approximately 12.5% total as compared to about 33.4 and 34.5% for used alumina from adsorption runs at 1.7 and 2.5 mL/min, respectively. It is important to note that a significant weight loss for the used samples occurred at temperature less than 200°C where activity-binding degradation products would desorb or burn off to carbon dioxide and other volatile compounds.

The TGA curves for used activated bauxite samples are shown in Fig. 3, along with the TGA curve for fresh bauxite sample; the used samples were obtained from adsorption column runs at two different flow rates. The TGA curves for bauxite samples were similar to those of the activated alumina, showing two plateaus for both used and fresh samples. The similarities of the TGA curves of the two adsorbents suggest that the same adsorption mechanism has taken place for activity-binding degradation products. The weight loss for the fresh activated bauxite was 12.6% total as compared to about 29.6 and 28.6% for the used samples obtained from 1.45 and 2.2 mL/min adsorption runs, respectively. It should be noted that much of the weight loss for the used samples again occurred at temperatures lower than 200°C as previously observed for the used activated alumina samples.

Experimental Breakthrough Curves

Experimental breakthrough curves of activity-binding degradation products on activated alumina and activated bauxite adsorbents are shown in Fig. 4, where the vertical axis represents the residual activity in effluent solvent in dpm/mL and the horizontal axis represents the time elapsed from initial contact of contaminated solvent with the adsorbent bed. It should be noted that the same weight of adsorbents (50 g) was used in each case at ambient conditions. The feed flow rate was maintained at 0.7 mL/min for these experiments. As can be seen from the figure, a general similarity of the breakthrough curves exists between activated alumina (Type A-2) and activated bauxite (Type RI) samples. This suggests that the chemical nature of the active sites responsible for adsorption

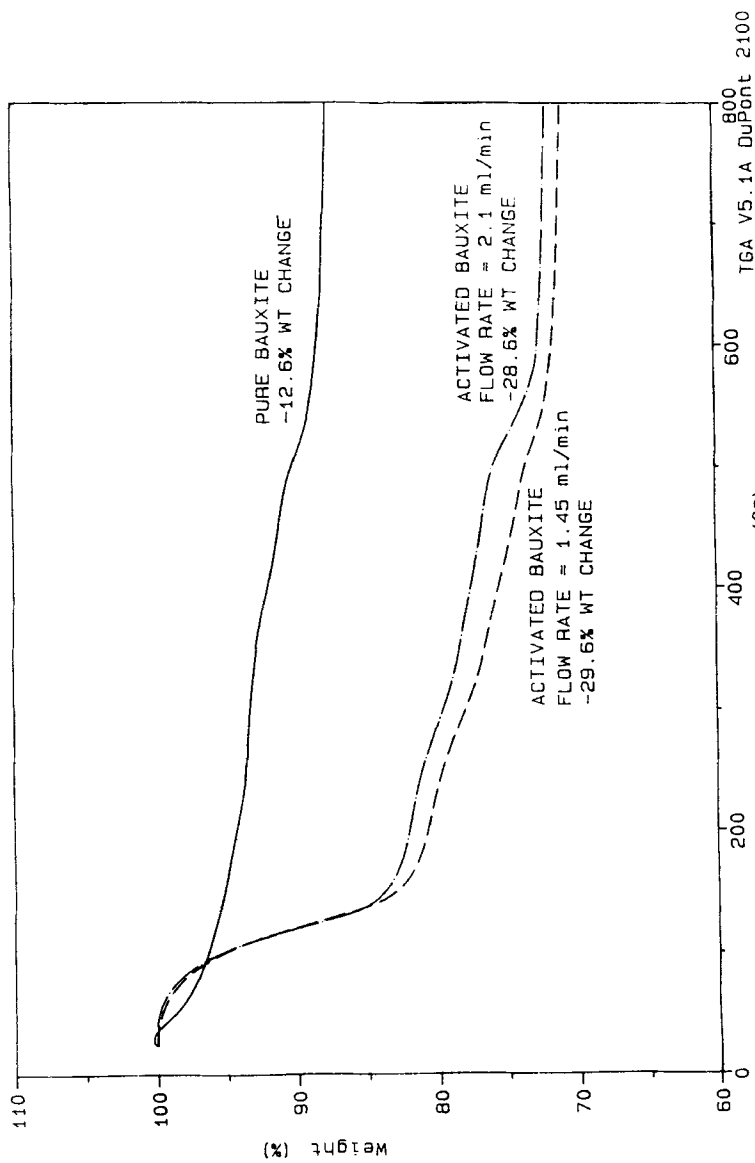

FIG. 3 TGA weight loss curves of activated bauxite samples.

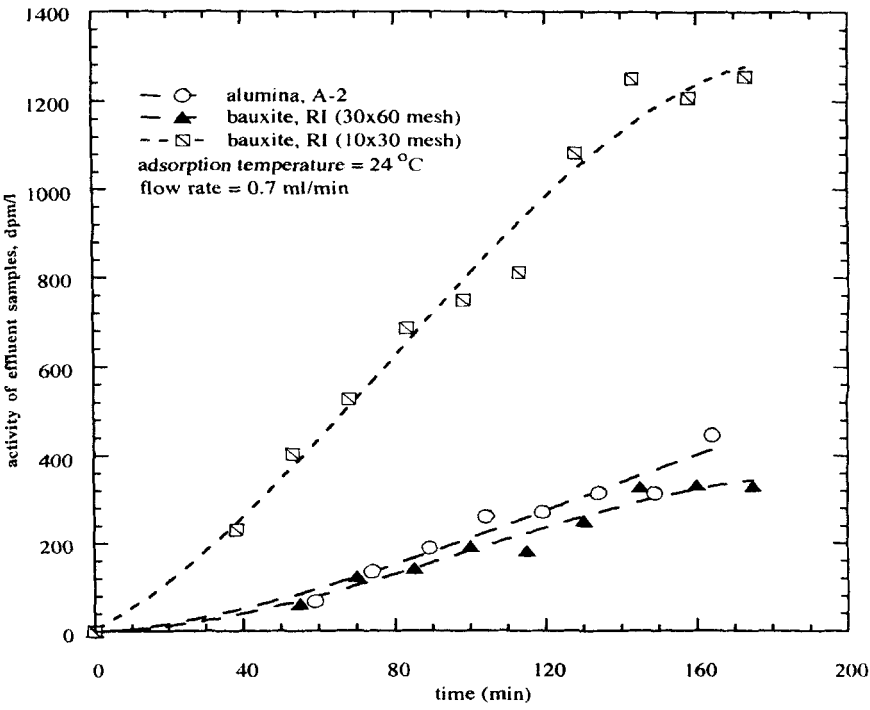

FIG. 4 Experimental breakthrough curves of degradation products on activated alumina and bauxite samples.

of degradation impurities on activated alumina was similar to that of activated bauxite. The adsorbents are considered to possess both Lewis and Bronsted acidic sites which tend to adsorb organic compounds by chemisorption (10, 11).

The temperature effects on adsorption of activity-binding degradation products on activated alumina are shown in Fig. 5. As shown in the figure, the residual activity in the effluent solvent decreases with increasing adsorption temperature, resulting in higher adsorption capacity of activated alumina. The temperature dependence of the present system is contrary to the physical adsorption phenomena in which higher adsorption temperatures will cause the adsorption capacity of the adsorbent to be reduced. Therefore, the adsorption of activity-binding degradation materials on activated alumina must have occurred by a chemisorption mechanism which is specific and occurs only on certain active sites by covalent bonding or by ionic association. The adsorption capacity of the alumina at 24, 42,

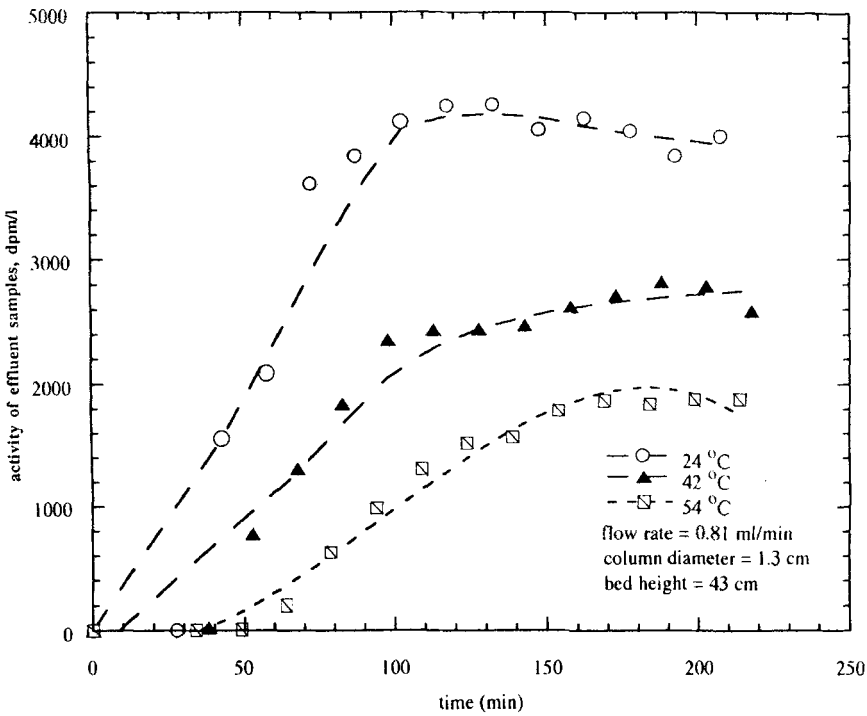

FIG. 5 Temperature effects on adsorption of degradation products on activated alumina.

and 59°C was found to be 1.05×10^4, 1.86×10^4, and 1.80×10^4 dpm/g, respectively. Table 3 shows that the calculated height of the adsorption zone decreases with increasing temperature and that the efficiency increases.

Figure 6 shows the effects of temperature on adsorption breakthrough curves of activity-binding degradation products on activated bauxite. As shown in the figure, the residual activity in the effluent solvent decreases with increasing temperature in the range from 26 to 69°C. The adsorption capacity of activated bauxite was found to be 1.92×10^5, 1.96×10^5, and 2.04×10^5 dpm/g at 26, 42, and 69°C, respectively. In Table 4 the calculated height and the efficiency of the adsorption zone are presented. Because different feed solvents and column sizes were used for activated alumina and bauxite systems, the merits of these results should be evaluated separately.

TABLE 3
Effects of Temperature on Process Dynamic Parameters for Adsorption of Degradation Products on Activated Alumina

Temperature (°C)	Height of adsorption zone (h_z, cm)[a]	Efficiency (γ, %) of adsorption zone	Dynamic capacity (q_m dpm/g adsorbent)
24	95.5	11.6	1.05×10^4
42	85.9	20.5	1.86×10^4
59	59.9	44.6	1.80×10^4

[a] Based on a total bed height of 43.7 cm with a column diameter of 13 mm.

The experimental breakthrough curves of activity-binding degradation products on activated alumina were obtained at three different feed flow rates, and the results are shown in Fig. 7. As shown in the figure, the activity of the effluent solvent increases with increasing flow rate at breakthrough. The process dynamic parameters presented in Table 5, however,

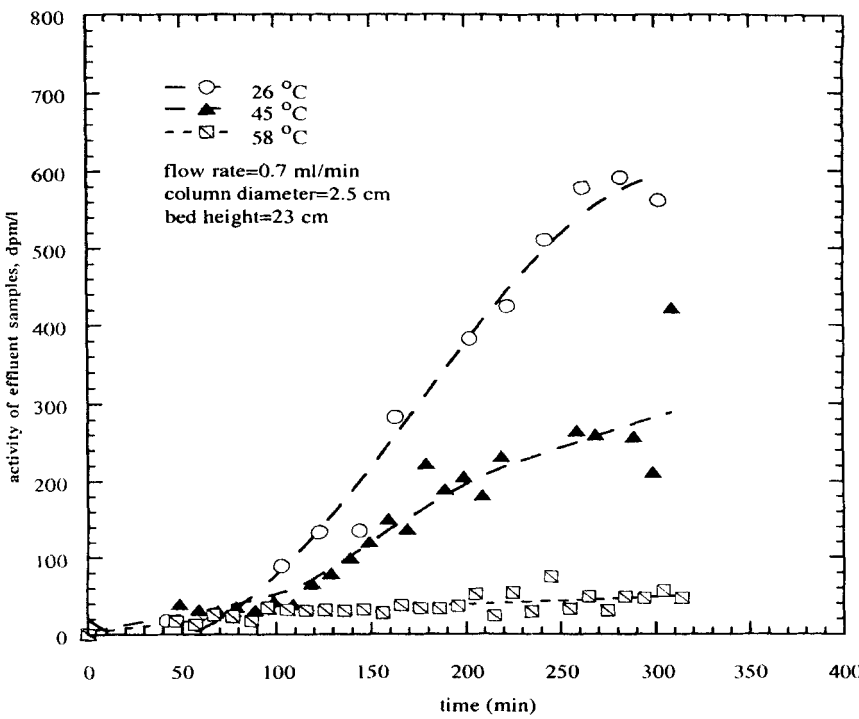

FIG. 6 Temperature effects on adsorption of degradation products on activated bauxite.

TABLE 4
Effects of Temperature on Process Dynamic Parameters for Adsorption of Degradation Products on Activated Bauxite

Temperature (°C)	Height of adsorption zone (h_z, cm)[a]	Efficiency (γ, %) of adsorption zone	Dynamic capacity (q_m dpm/g adsorbent)
26	19.6	65.8	1.92×10^5
42	24.1	57.8	1.96×10^5
69	23.1	59.5	2.04×10^5

[a] Based on a total bed height of 22.9 cm with a column diameter of 25 mm.

show a maximum column performance at 1.7 mL/min, where the dynamic capacity of activated alumina is 1.28×10^4 dpm/g and the height and efficiency of the adsorption zone are 84.5 cm and 21.7%, respectively. Because the calculated height of the adsorption zone was nearly twice the adsorbent bed, an additional quantity of adsorbent was required to compensate for the presence of the adsorption zone.

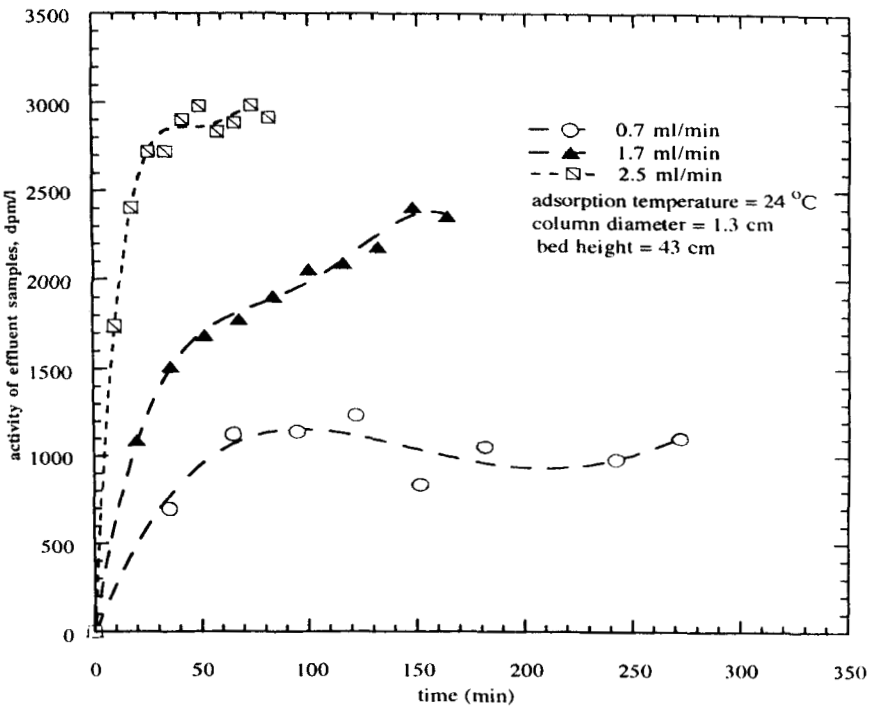

FIG. 7 The effects of flow rate on breakthrough curves of degradation products on activated alumina.

TABLE 5
Effects of Flow Rate on Process Dynamic Parameters for Adsorption of Degradation Products on Activated Alumina

Flow rate (mL/min)	Height of adsorption zone (h_z, cm)[a]	Efficiency (γ, %) of adsorption zone	Dynamic capacity (q_m dpm/g adsorbent)
0.7	88.0	18.5	6.65×10^3
1.7	84.5	21.7	1.28×10^4
2.5	93.8	13.2	7.02×10^3

[a] Based on a total bed height of 43.7 cm with a column diameter of 13 mm.

Figure 8 shows the breakthrough curves of degradation products on activated bauxite at three different flow rates. The effects of the flow rate on the process dynamic parameters are shown in Table 6. It should be noted that the dynamic capacity of activated bauxite decreases with increasing flow rate, as expected. The calculated values were 1.37×10^5,

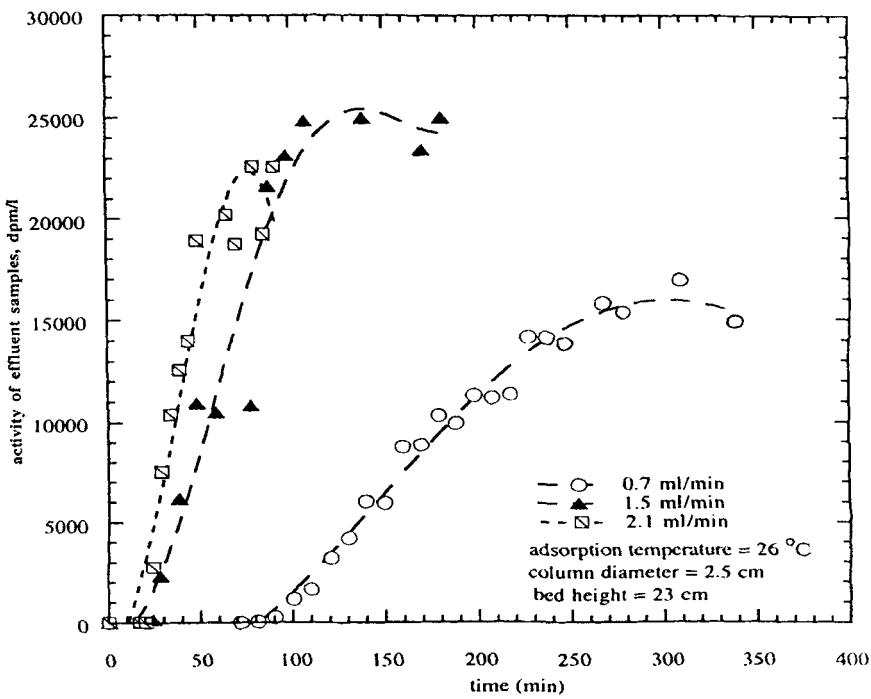

FIG. 8 The effects of flow rate on breakthrough curves of degradation products on activated bauxite.

TABLE 6
Effects of Flow Rate on Process Dynamic Parameters for Adsorption of Degradation Products on Activated Bauxite

Flow rate (mL/min)	Height of adsorption zone (h_z, cm)[a]	Efficiency (γ, %) of adsorption zone	Dynamic capacity (q_m dpm/g adsorbent)
0.8	21.3	62.5	1.37×10^5
1.45	35.1	38.5	1.27×10^5
2.1	33.3	41.9	1.26×10^5

[a] Based on a total bed height of 22.9 cm with a column diameter of 25 mm.

1.27×10^5, and 1.26×10^5 dpm/g for the flow rates 0.8, 1.45, and 2.1 mL/min, respectively. The efficiency of the adsorption zone dropped from 62% to less than 40%. Although these results show an expected trend, further optimization of the process operating parameters are needed for each particular waste solvent and adsorbent material.

CONCLUSION

An adsorption process was evaluated for decontamination of radioactive waste solvent from the Purex process. The process utilized two commercially available adsorbents for the removal of activity-binding degradation products from radioactive waste solvent. Experimental breakthrough curves were obtained from various column runs under a wide range of operating temperatures and flow rates. The results from the experimental studies show the following.

1. The use of activated alumina and activated bauxite adsorbents can achieve the removal of activity-binding secondary degradation products from waste solvent in a one-cycle process.
2. Thermogravimetric analyses of activated alumina and bauxite samples show a similarity of adsorption mechanisms for the two adsorbents.
3. The dynamic capacities of activated alumina and activated bauxite increase with adsorption temperature in the range from about 24 to 70°C and decrease with increasing feed flow rate.
4. The performance of the adsorption decontamination process can be correlated with experiment-based process dynamic parameters.

ACKNOWLEDGMENTS

This work was supported by the US Department of Energy under Contract DE-AC09-89SR18035 with Westinghouse Savannah River Co. We

gratefully acknowledge La Roche Chemicals for providing the activated alumina samples and Engelhard Chemical Co. for providing the activated bauxite samples. We are indebted to Yvonne J. Simpkins and Kevin J. Kalbaugh for their assistance in the experimental work.

REFERENCES

1. E. S. Lane, *Nucl. Sci. Eng.*, *17*, 620 (1963).
2. J. C. Neace, *Sep. Sci. Technol.*, *18*, 1581 (1983).
3. O. K. Tallent, J. C. Mailen, and K. E. Dodson, *Nucl. Technol.*, *71*, 417 (1985).
4. Y. Sze, T. E. McDougall, and C. G. Martin, *Solv. Extr. Ion Exch.*, 5(1), 129 (1987).
5. F. Secilio, T. H. Goodgame, and B. Wilkins, *Nucl. Sci. Eng.*, *9*, 455 (1961).
6. C. A. Blake, W. Davis, and J. M. Schmitt, *Ibid.*, *17*, 626 (1963).
7. D. J. Reif, *Nucl. Technol.*, *83*, 190 (1988).
8. J. C. Mailen, *Ibid.*, *83*, 182 (1988).
9. A. S. Michael, *Ind. Eng. Chem.*, *44*(8), 1922 (1952).
10. R. Desi, M. Hussein, and D. M. Ruthven, *Can. J. Chem. Eng.*, *70*, 699 (1992).
11. H. Tamon, S. Koyotani, and H. Wada, *J. Chem. Eng. Jpn.*, *14*, 136 (1981).

Received by editor October 3, 1994